Facile fabrication, properties and application of novel thermo-responsive hydrogel

2011 Smart Mater. Struct. 20 075005

(http://iopscience.iop.org/0964-1726/20/7/075005)

Smart Mater. Struct. **20** (2011) 075005 (7pp) doi:10.1088/0964-1726/20/7/075005

Facile fabrication, properties and application of novel thermo-responsive hydrogel

Jiaxing Li[1,2], Xiuqing Gong[1], Xin Yi[1], Ping Sheng[1] and Weijia Wen[1]

[1] Department of Physics and Institute of Nano Science and Technology, The Hong Kong University of Science and Technology, Clear Water Bay, Kowloon, Hong Kong
[2] Key Laboratory of Novel Thin Film Solar Cells, Institute of Plasma Physics, Chinese Academy of Sciences, PO Box 1126, 230031, Hefei, People's Republic of China

E-mail: phwen@ust.hk

Received 21 February 2011, in final form 5 May 2011
Published 31 May 2011
Online at stacks.iop.org/SMS/20/075005

Abstract
The authors report a novel thermo-responsive hydrogel design based on the thermally induced aggregation of two kinds of nonionic surfactants: triblock copolymer poly(ethylene oxide)–poly(propylene oxide)–poly(ethylene oxide) (EPE) and 4-octylphenol polyethoxylate (TX-100). In the preparation of the hydrogel, agarose is used to host the aqueous surfactant molecules, allowing them to move freely through its intrinsic network structure. To study it, EPE molecules are labeled with fluorescent Rhodamine B, and the aggregation phenomenon under various temperatures is imaged by fluorescence microscopy. In order to realize flexible control of the opaque/transparent transition temperature (OTTT), the surfactants' aggregation is modified by adding ionic surfactant or salts. The rate of the opaque/transparent transition and applications in the smart window and smart roof based on this kinds of hydrogel are also investigated.

(Some figures in this article are in colour only in the electronic version)

1. Introduction

Recent advances in intelligent hydrogels have resulted in new materials that have found applications in many areas of materials science [1–13]. Novel applications presently being considered for thermochromic materials are thermally adjustable smart windows, smart roofs, large-area information displays and traffic engineering, as well as temperature-sensing applications in medical technologies [14–16]. This is one of the most promising applications of what are called intelligent hydrogels, based on their opaque/transparent-reversibility property for temperature or electric fields, which can control the passage of light. In the last decade, reversible thermochromic hydrogels sensitive to external temperature have been extensively investigated, though, with the exception of poly(N-isopropylacrylamide) (PNIPAAm) hydrogel, they have only rarely been analyzed. PNIPAAm hydrogel, from which many kinds of hydrogels have been derived, is the best known temperature-sensitive polymeric network [3–10]. All of these hydrogels present properties of volume phase transitions when either the temperature or pH changes [4, 11–14]. Recently, Ling *et al* reported a brine-prepared PNIPAAm hydrogel that undergoes transparent–opaque transitions with increasing NaCl concentration [3]. Unfortunately, this kind of high-NaCl hydrogel breaks into pieces due to its poor strength and volume phase transition. Yang *et al* investigated a novel thermo-responsive supramolecular hydrogel consisting of cucurbit[6]uril and butan-1-aminium 4-methylbenzenesulfonate, which together effect a gel (opaque)–sol (transparent) transition with temperature [15]. Seeboth and Chung developed a type of hydrogel that, by means of dye embedded in the polyvinyl alcohol/borax/surfactant gel network, responds to temperature changes with reversible color transformations [16, 17].

Agarose, a familiar hydrogel base, is a linear polymer made up of repeating monomeric units of agarobiose. The molecular structure of this polysaccharide, double helices formed of left-handed threefold helices, imparts the capacity

to form gels that are very strong, even at low concentrations. These double helices are stabilized by the presence inside their cavities of bound water molecules [18, 19]. Exterior hydroxyl groups allow the aggregation of up to 10 000 of these helices to form suprafibers and, thereby, stable hydrogel.

All thermally induced hydrogels have many advantages including high transparency, freedom from an organic solvent, non-flammability, biodegradability, and others. However, they are often high cost, difficult to fabricate, volume phase change, and narrow transition temperature range. To remedy this problem, we formulated a stable, innocuous, easily adjustive and completely biodegradable hydrogel using cheap and readily available industrial materials.

2. Experimental section

2.1. Chemical materials

Agarose (the hydrogel base); poly(ethylene oxide)-poly(propylene oxide)–poly(ethylene oxide) (EPE) (total average molecular weight: 2000; molecular PEO weight: 1600) and 4-octylphenol polyethoxylate (TX-100) (the surfactants); sodium dodecyl sulfate (SDS) and sodium sulfate (the additives); Rhodamine B. All of these chemicals, purchased from Sigma-Aldrich, were analytical grade and used without further purification.

2.2. Preparation

Preparation of the agarose, surfactants and additives stock solution. The stock solutions containing 2 w/v% agarose, 2 w/v% surfactant EPE, 5 w/v% TX-100, 1 w/v% SDS, 5 M Na_2SO_4 were further diluted with deionized water to the required concentrations in preparing the hydrogels.

2.3. Synthesis of hydrogels

The hydrogels were synthesized by mixing hot surfactant, agarose, and additive solutions to different ratios under stirring and sonication. The transparent hydrogels formed after the mixed solutions were left to cool (without stirring).

2.4. Measurements

The temperatures were measured with a digital thermal meter, and the absorption spectra were obtained with a Lambda 20 (Perkin Elmer) UV–Visible spectrometer. The fluorescence was imaged under an inverted fluorescence microscope (Axiovert 200 M, Zeiss) equipped with a cooled charge-coupled device camera (Diagnostic Instruments). All transparency of the hydrogel was measured after the sample was equilibrated at the expected temperature for 5 minutes. The thermal transport on the surface was measured using a thermo camera (FLIR ThermoVision A40).

3. Results and discussion

We chose as the support matrix agarose, a linear polymer composed of repeating monomeric units of agarobiose. Agarose is insoluble in cold water but in boiling water dissolves, yielding random coils. Gelation has been reported to follow a phase separation process and association on cooling (∼35 °C), forming gels of up to 99.5% water that remain solid up to about 85 °C [18–20]. In the present study, we used 0.5 w/v% agarose solution as the hydrogel base. Agarose is the most popular medium for electrophoresis for it has a large size for rapid diffusion and low background visibility [20, 21]. The pore size of the agarose gel, related with its concentration and temperature, ranges from 400 to 1200 nm at different temperatures when its concentration is 0.5 w/v% [19]. Therefore, the surfactants, additives or fluorescent molecules can disperse uniformly in the gel network of agarose (figures 1(b) and (c)).

In preparing the thermally induced hydrogel, we incorporated nonionic surfactants into the agarose network [21]. The principle of a thermally induced reversible hydrogel is straightforward. In the preparation of EPE hydrogel, hot nonionic surfactant EPE solution (turbid) is mixed with hot agarose solution. Then the uniform solution was cooled to room temperature without stirring for over 20 min, and solidified into hydrogel. At low temperatures, the nonionic surfactants, as individual molecules, are dissolved completely in the water of the hydrogel (figure 1(b)). When the hydrogel is heated, the surfactant molecules, owing to the dehydration of the hydrophobic groups, begin to form micelles dispersed uniformly in the hydrogel matrix and to undergo phase separation [22, 23]. If the hydrogel is heated to the opaque/transparent transition temperature (OTTT), neighboring micelles aggregate into larger clusters (figure 1(c)), the morphology of which is the cause of the turbid appearance. The whole process completed within half a minute including the heating time. At higher and equal OTTT, complete hydrogel opaqueness, which blocks radiation such as sunlight. To verify the micelles' larger cluster formations, we dissolved a trace amount of Rhodamine B (red fluorescence) into the water of the hydrogel during the preparation process and then imaged the fluorescence under an inverted fluorescence microscope. Rhodamine B is the source of the hydrogel's affinity for surfactant molecules, which is also the rationale for its use in surfactant phase labeling [24]. Next, the hydrogel was laid on an ITO glass connected to heating electrodes. We took 3D hydrogel images (200 μm × 200 μm × 20 μm) at low and high temperature. Below the OTTT, there were no distinct fluorescent spots detected (figure 1(e)). Above the OTTT, 55 °C, many distinct micron fluorescent clusters were observed quickly within one second as the individual surfactants became micelle clusters (figure 1(d)), which eventually produced the turbidity. Such a phenomenon was reversible if the temperature variation was reversed. When the whole sample was cooled to 25 °C, those fluorescent clusters disappeared within 1 s.

To enable flexible cloud point (CP) control, we variably charged the nonionic surfactant by adding ionic surfactants or salt. It is well known that nonionic surfactants in the aqueous solution phase separate at the CP [25], this process involves a drastic increase in the turbidity of the solution, which influences the light transmittance. The CP of nonionic surfactants is very sensitive to interaction between molecules,

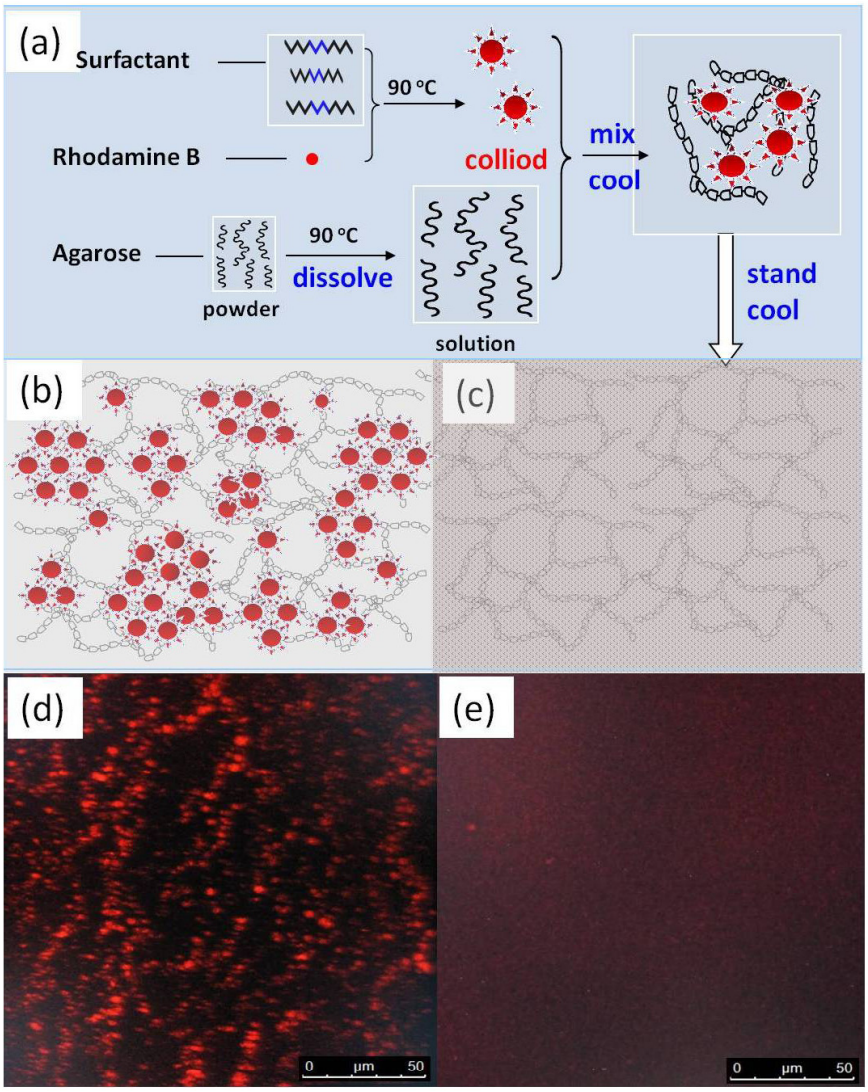

Figure 1. (a) Preparation procedures of agarose-based thermo-sensitive hydrogel: the agarose was dissolved in hot water to form an aqueous solution, and then hot surfactant and Rhodamine B colloid suspension was added, stirred, and let stand while cooling. (b) Outline of hydrogel-containing Rhodamine B at 55 °C (high temperature). (c) Outline of hydrogel-containing Rhodamine B at 25 °C (low temperature). (d) In the aggregated surfactant micelles the density of Rhodamine B molecules is higher at a high temperature (55 °C), which produces fluorescent spots under fluorescence microscopy. (e) Aggregation of surfactant micelles is absent at low temperature (25 °C) so that Rhodamine B molecules are uniform in the region, which means no fluorescent spots can be detected.

and also affected by other chemicals [25–32]. The effect of added salt and ionic surfactants on the CP of nonionic surfactants has already been investigated [23, 33, 34]. In the present study, we investigated two kinds of nonionic surfactant, EPE and TX-100. These two molecules, containing both hydrophobic and hydrophilic groups, can, owing to the dehydration of hydrophobic groups at a certain temperature, self-assemble to form micelles in aqueous solution. We used two kinds of additive to tune the CP of the two surfactants so that the OTTT of the hydrogel can be controlled. The anion surfactant, SDS, can increase the CP temperature of EPE [23, 33], while the salt, Na_2SO_4, can depress the CP temperature of TX-100 [28, 29].

To determine the viability of the hydrogel transparency control, for the EPE hydrogel we used 1 w/v% EPE, with different concentrations of SDS added to a 0.5 w/v% agarose solution base, as the medium to control the passage of light through the 2 mm thick hydrogel membrane. As for the EPE hydrogel without SDS, at 25 °C it maintained perfect transparency while it was completely opaque at 30 °C (figure 2(c)). After 0.6 w/v% SDS was added, the OTTT was increased to 55 °C as shown in the insets of figure 2(a). From 25 °C to 48 °C the transparency did not change appreciably, and the hydrogel retained the same appearance as the pure agarose hydrogel. However, at 52 °C some turbidity could be observed, and after the temperature was raised to 55 °C, the hydrogel became completely light-tight (inset images in figure 2(a)). For the TX-100 hydrogel, we used 2 w/v% TX-100 solution containing Na_2SO_4 with different contents. The OTTT of pure TX-100 hydrogel (∼70 °C) is much higher than that of pure EPE hydrogel (27 °C). Below 300 nm, the transmission through TX-100 hydrogel, unlike the EPE type,

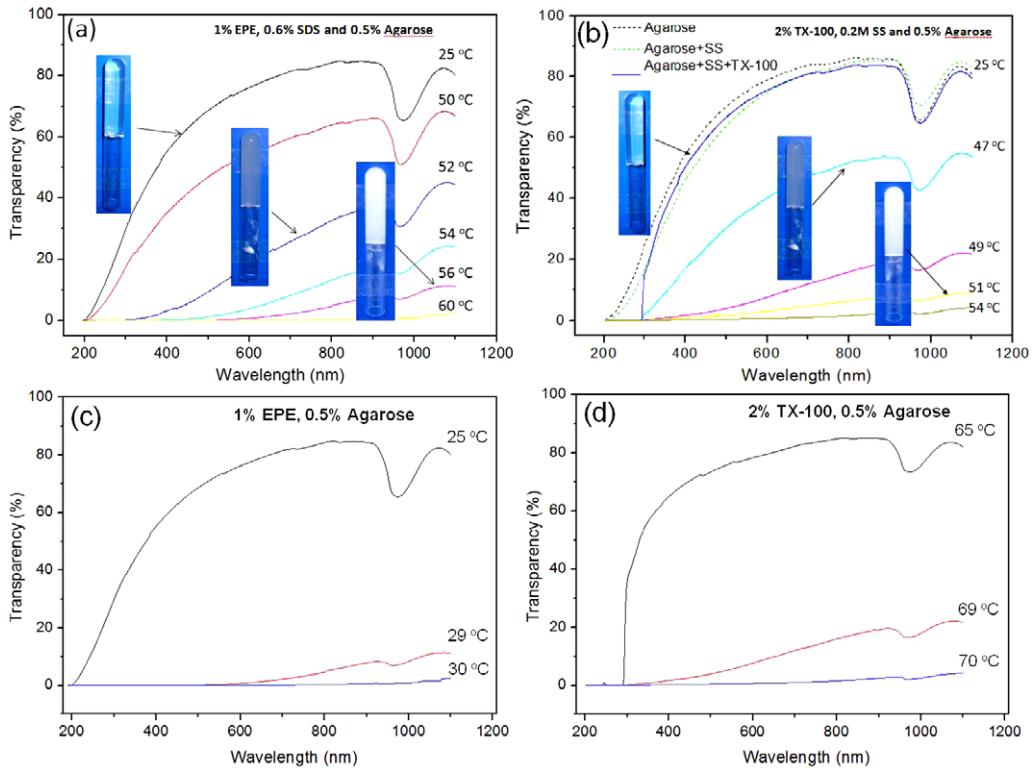

Figure 2. (a) Temperature dependence of transparency of the sample (1 w/v% EPE, 0.6 w/v% in 0.5 w/v% agarose hydrogel). (b) Temperature dependence of transparency of the sample (2 w/v% TX-100, 0.2 M SS in 0.5 w/v% agarose hydrogel). In both (a) and (b), the insets show the hydrogel in a glass tube at different temperatures. (c) 1 w/v% EPE in 0.5 w/v% agarose hydrogel. (d) 2% TX-100 in 0.5 w/v% agarose hydrogel.

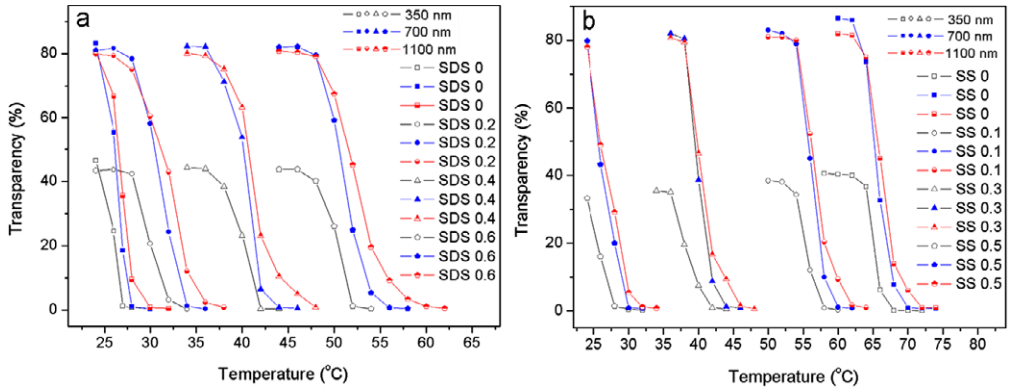

Figure 3. (a) Influence of SDS concentrations on transmittance of EPE hydrogel, and (b) influence of SS concentrations on transmittance of TX-100 hydrogel, both measured at 350, 700, and 1100 nm wavelengths.

is totally blocked due to absorption (figure 2(b)). The TX-100 hydrogel is perfectly transparent at 68 °C and completely opaque at 70 °C (figure 2(d)). When 0.2 M Na_2SO_4 was added to this hydrogel, its OTTT fell to ∼54 °C. The hydrogel transparency diminishes with a gradually increasing temperature but is recoverable if the temperature decreases again. Based on this property, hydrogels can be employed as media for control of the passage of light through the smart window or roof, which utility we studied.

We mixed 0.1–0.7 w/v% SDS into the EPE hydrogel base, and 0.1–0.6 M Na_2SO_4 into the TX-100 hydrogel base, respectively. The sunscreen efficiency of the hydrogel was determined by measuring the light transmittance as a function of temperature at 350, 700 and 1100 nm wavelengths (figure 3). For both hydrogels, the transparency at 350 nm was less than 50%, much lower than those measured at 700 and 1100 nm. The region from the maximum transparency temperature to the minimum increased with the wavelength (350 nm < 700 nm < 1100 nm). To illustrate the effect of SDS and Na_2SO_4 in improving or depressing the OTTT, the opaque temperature as a function of SDS/Na_2SO_4 concentration is plotted in figure 4. With increasing SDS concentration, the temperature at which the EPE hydrogel attained its opaque state was shifted markedly higher, but with increasing Na_2SO_4 concentration,

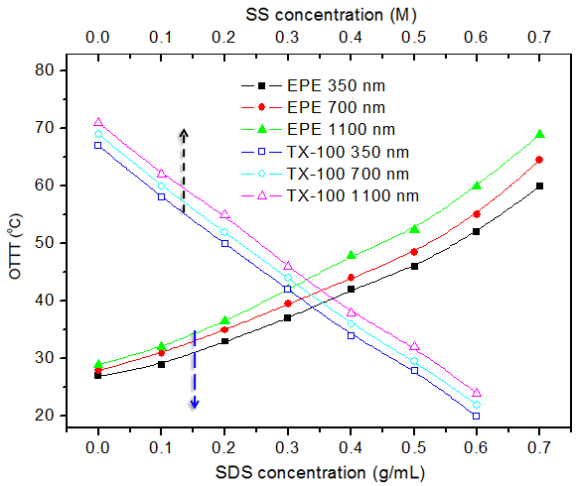

Figure 4. Influence of additives (SDS, Na_2SO_4) concentration on opaque temperature of hydrogel measured at 350, 700 and 1100 nm wavelengths.

that of the TX-100 hydrogel was shifted downward. It can be seen that the OTTT of both hydrogels is lower at short wavelengths, and that the OTTT gaps between both of the two sets of neighbored wavelengths of the EPE hydrogel are larger than those for the TX-100 hydrogel. OTTT modification was shown, thus, to be a potential means of actively controlling the passage of light through the hydrogel. Through this method, we can obtain the desired OTTT for different hydrogels.

Hydrogel becomes reversibly more and more opaque as it is heated. The rate of the opaque/transparent transition is a function not only of the properties of the surfactant but also of the thermal conductivity of the hydrogel. Preparatory to studying surface thermal transport, a piece of hydrogel (∼20 °C) was attached to a large-capacity thermal source applying a constant temperature (∼75 °C). The temperature of the hydrogel surface was measured using a thermo camera. The experiment results are summarized in figure 5. It is apparent that the thermal transport distance increases with time (see the insets) and that the temperature decreases with increasing distance from the source. In figure 5(b), the temperature evolutions are shown at four points laying at different distances

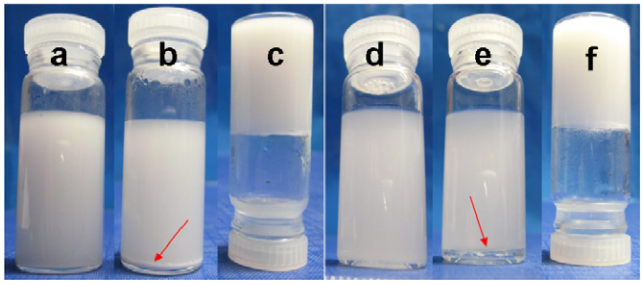

Figure 6. Photos of 1% EPE, 0.3% SDS solution at 50 °C (a) 5 min, (b) 8 h, 1% EPE, (c) 0.3% SDS and 0.5% agarose hydrogel at 50 °C 8 h, 2% TX-100, 0.3 M Na_2SO_4 at 50 °C, (d) 5 min (e) 8 h, (f) 2% TX-100, 0.3 M Na_2SO_4 and 0.5% agarose hydrogel at 50 °C 8 h.

from the thermal source. It can be seen that the temperatures arrive at equilibrium within half a minute for this sample while it has a complete transition in nearly the same period of time, which means that thermal transport mainly effects the speed of the hydrogel's opaque/transparent transition.

Compared with solution-based thermally induced material, solid hydrogel is much more stable. Sedimentation occurs in colloidal systems because of the density mismatch between different phases, as accentuated by particles (micelle clusters) aggregation. It can be seen in figure 6 that the solution sample at 50 °C was a uniform milk-white emulsion (figure 6(a): EPE/SDS solution; figure 6(d): TX-100/Na_2SO_4 solution) at the beginning, whereas after letting it stand for 8 h, there was some white (figure 6(b): EPE/SDS solution) or transparent (figure 6(e): TX-100/Na_2SO_4 solution) deposition at the bottom of the bottle. These results reflected the fact that surfactant micelles at high temperature aggregate clusters and get larger and larger, undergo phase separation and slowly sink to the bottom over time. Hydrogel, in contrast, is almost unchanged after even several days, due to the gel networks of agarose preventing the aggregation of large micelle clusters (figures 6(c) and (f)). The agarose is not only the base of the hydrogel but also the basal network that stabilizes the emulsion.

We used the hydrogel as a medium to control the passage of light through a smart window. In order to demonstrate the light screen, a piece of hydrogel membrane (2 mm thickness)

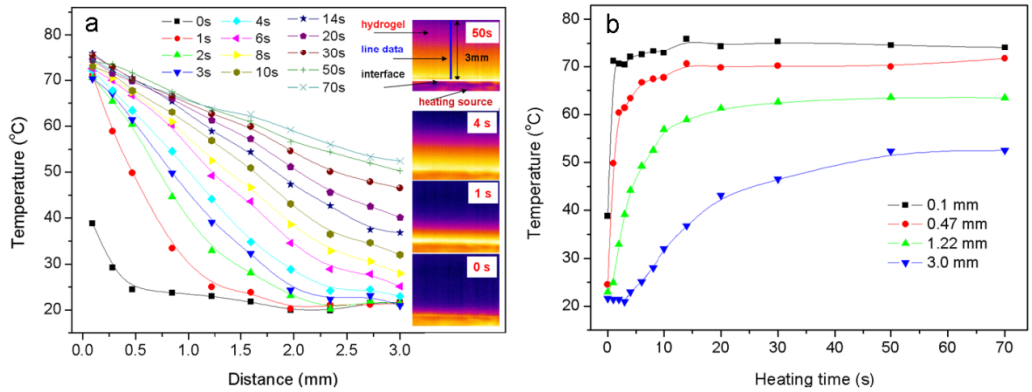

Figure 5. Thermal conductivity of hydrogel. (a) Temperature at different heating times as function of distances, (b) temperature at different positions as function of heating time.

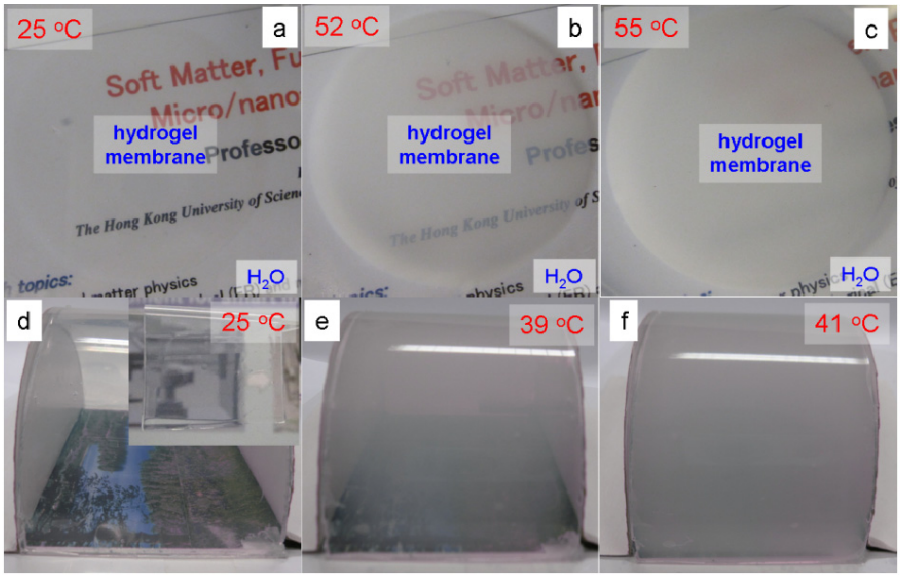

Figure 7. Smart hydrogel membranes at different temperatures, hydrogel membranes in water at (a) 25 °C, (b) 52 °C, (c) 55 °C, model of greenhouse at (d) 25 °C (inset image is of piece of hydrogel membrane), (e) 39 °C, (f) 41 °C.

was immersed into water and a paper with different color words was placed under the transparent water container. The temperature of the hydrogel was controlled by the water in the container. At room temperature, the hydrogel membrane was transparent and the colored words, accordingly, were clearly visible (figure 7(a)). But when the room-temperature water was exchanged for 52 °C hot water (near the OTTT), the resultant turbidity imparted cloudiness to the membrane within half a minute, and the profile of the colored words became obscure (figure 7(b)). Once the temperature exceeded the OTTT (55 °C), the hydrogel membrane screened most of the light, becoming completely opaque within half a minute, no background being visible (figure 7(c)). This process is reversible: when the temperature of the water cools to room temperature, the hydrogel membrane will recover its transparent state within several minutes, according to how fast the temperature can be lowered. Utilizing this reversibility property, we used the membrane as either a thermo-sensitive smart window or smart roof of a greenhouse (figures 6(d) and (e)).

4. Conclusions

A new, thermo-responsive and tunable hydrogel system was rapidly built from agarose gel networks containing nonionic surfactants and additives, which are very cheap and common industrial materials offering excellent biocompatibility and biodegradability. It is likely that other thermally sensitive functional materials will manifest similar behavior in hydrogel networks. The interesting thermal and optical phenomena of this kind of hydrogel indicate that further investigation of the physical properties and the possible applications of these materials is merited. In the future, these high-transparency hydrogels will serve as economical substitutes in electrochromic [35] and photochromic [36, 37] applications such as large-scale sun-blocking smart windows or the roofs of greenhouses.

Acknowledgments

The authors would like to acknowledge Hong Kong RGC grants HKUST 602207, 621006 and 603608 for the financial support of this project. The work was also partially supported by the Nanoscience and Nanotechnology Program at HKUST.

References

[1] Lee Y, Chung H J, Yeo S, Ahn C H, Lee H, Messersmith P B and Park T G 2010 Thermo-sensitive, injectable, and tissue adhesive sol–gel transition hyaluronic acid/pluronic composite hydrogels prepared from bio-inspired catechol-thiol reaction *Soft Matter* **6** 977–83

[2] Gong C Y *et al* 2007 A thermosensitive hydrogel based on biodegradable amphiphilic poly(ethylene glycol)–polycaprolactone–poly(ethylene glycol) block copolymers *Smart Mater. Struct.* **16** 927–33

[3] Ling Y D and Lu M G 2009 Thermo and pH dual responsive poly(*N*-isopropylacrylamide-co-itaconic acid) hydrogels prepared in aqueous NaCl solutions and their characterization *J. Polym. Res.* **16** 29–37

[4] Kim S J, Kim H I, Park S J, Kim I Y, Lee S H, Lee T S and Kim S I 2005 Behavior in electric fields of smart hydrogels with potential application as bio-inspired actuators *Smart Mater. Struct.* **14** 511–4

[5] Zhang J, Chu L Y, Li Y K and Lee Y M 2007 Dual thermo- and pH-sensitive poly(*N*-isopropylacrylamide-co-acrylic acid) hydrogels with rapid response behaviors *Polymer* **48** 1718–28

[6] Yan S F, Yin J B, Yu Y, Luo K and Chen X S 2009 Thermo- and pH-sensitive poly(vinylmethyl ether)/carboxymethylchitosan hydrogels crosslinked using electron beam irradiation or using glutaraldehyde as a crosslinker *Polym. Int.* **58** 1246–51

[7] Moon J R and Kim J H 2008 Biodegradable thermo- and pH-responsive hydrogels based on amphiphilic polyaspartamide derivatives containing *N*,*N*-diisopropylamine pendants *Macromol. Res.* **16** 489–91

[8] Chen J P and Cheng T H 2009 Preparation and evaluation of thermo-reversible copolymer hydrogels containing chitosan and hyaluronic acid as injectable cell carriers *Polymer* **50** 107–16
[9] Chacon D, Hsieh Y L, Kurth M J and Krochta J M 2000 Swelling and protein absorption/desorption of thermo-sensitive lactitol-based polyether polyol hydrogels *Polymer* **41** 8257–62
[10] Ueno K, Matsubara K, Watanabe M and Takeoka Y 2007 An electro- and thermochromic hydrogel as a full-color indicator *Adv. Mater.* **19** 2807–12
[11] Tasdelen B, Kayaman-Apohan N, Guven O and Baysal B M 2004 Investigation of drug release from thermo- and pH-sensitive poly(*N*-isopropylacrylamide/itaconic acid) copolymeric hydrogels *Polym. Adv. Technol.* **15** 528–32
[12] Schmaljohann D, Oswald J, Joergensen B, Nitschke M, Beyerlein D and Werner C 2003 Thermo-responsive hydrogels for controlled cell adhesion and detachment *Abstr. Pap. Am. Chem. Soc.* **226** U484
[13] Morimoto N, Ohki T, Kurita K and Akiyoshi K 2008 Thermo-responsive hydrogels with nanodomains: rapid shrinking of a nanogel-crosslinking hydrogel of poly(*N*-isopropyl acrylamide) *Macromol. Rapid Comm.* **29** 672–6
[14] Lang Y Y, Li S M, Pan W S and Zheng L Y 2006 Thermo- and pH-sensitive drug delivery from hydrogels constructed using block copolymers of poly(*N*-isopropylacrylamide) and Guar gum *J. Drug Deliv. Sci. Technol.* **16** 65–9
[15] Yang H, Tan Y B and Wang Y X 2009 Fabrication and properties of cucurbit[6]uril induced thermo-responsive supramolecular hydrogels *Soft Matter* **5** 3511–6
[16] Seeboth A, Kriwanek J and Vetter R 1999 The first example of thermochromism of dyes embedded in transparent polymer gel networks *J. Mater. Chem.* **9** 2277–8
[17] Lee S M, Chung W Y, Kim J K and Suh D H 2004 A novel fluorescence temperature sensor based on a surfactant-free PVA/borax/2-naphthol hydrogel network system *J. Appl. Polym. Sci.* **93** 2114–8
[18] Labropoulos K C, Niesz D E, Danforth S C and Kevrekidis P G 2002 Dynamic rheology of agar gels: theory and experiments. Part I. Development of a rheological model *Carbohydr. Polym.* **50** 393–406
[19] Narayanan J, Xiong J Y and Liu X Y 2006 Determination of agarose gel pore size: Absorbance measurements vis a vis other techniques *J. Phys.: Conf. Ser.* **28** 83–6
[20] Matsuo M 2005 Reply to the paper 'Comment on Gelation mechanism of agarose and kappa-carrageenan solutions estimated in terms of concentration fluctuation' [Polym 2002; 43: 5299] *Polymer* **46** 3538
[21] Ivory C F 1988 The prospects for large-scale electrophoresis *Sep. Sci. Technol.* **23** 875–912
[22] Guo C, Wang J, Liu H Z and Chen J Y 1999 Hydration and conformation of temperature-dependent micellization of PEO–PPO–PEO block copolymers in aqueous solutions by FT-Raman *Langmuir* **15** 2703–8
[23] Gong X Q, Li J X, Chen S Y and Wen W J 2009 Copolymer solution-based 'smart window' *Appl. Phys. Lett.* **95** 2519071
[24] Cho H K, Cho K S, Cho J H, Choi S W, Kim J H and Cheong I W 2008 Synthesis and characterization of PEO–PCL–PEO triblock copolymers: effects of the PCL chain length on the physical property of W-1/O/W-2 multiple emulsions *Colloids Surf.* B **65** 61–8
[25] GaleraGomez P A and Gu T 1996 Cloud point of mixtures of polypropylene glycol and triton X-100 in aqueous solutions *Langmuir* **12** 2602–4
[26] Schott H 1995 Effect of inorganic additves on solutions of nonionic surfactants. 10. Miccellar properties *J. Colloid Interface Sci.* **173** 265–77
[27] Schott H 1997 Effect of inorganic additives on solutions of nonionic surfactants. 15. Effect of transition metal salts on the cloud point of octoxynol 9 (Triton X-100) *J. Colloid Interface Sci.* **192** 458–62
[28] Schott H 1997 Effect of inorganic additives on solutions of nonionic surfactants. 14. Effect of chaotropic anions on the cloud point of octoxynol 9 (Triton X-100) *J. Colloid Interface Sci.* **189** 117–22
[29] Schott H 1998 Comparing the surface chemical properties and the effect of salts on the cloud point of a conventional nonionic surfactant, octoxynol 9 (Triton X-100), and of its oligomer, tyloxapol (Triton WR-1339) *J. Colloid Interface Sci.* **205** 496–502
[30] Schott H 2001 Effect of inorganic additives on solutions of nonionic surfactants—XVI. Limiting cloud points of highly polyoxyethylated surfactants *Colloids Surf.* A **186** 129–36
[31] Sharma K S, Patil S R and Rakshit A K 2003 Study of the cloud point Of C12En nonionic surfactants: effect of additives *Colloids Surf.* A **219** 67–74
[32] Aswal V K, Goyal P S, Kohlbrecher J and Bahadur P 2001 SANS study of salt induced micellization in PEO–PPO–PEO block copolymers *Chem. Phys. Lett.* **349** 458–62
[33] Chen S, Yang B, Guo C, Ma J H, Yang L R, Liang X F, Hua C and Liu H Z 2008 Spontaneous vesicle formation of poly(ethylene oxide)-poly(propylene oxide)-poly(ethylene oxide) triblock copolymer *J. Phys. Chem.* B **112** 15659–65
[34] Schott H 1997 Similarity between the clouding of nonionic surfactants and the denaturation of biopolymers, and the effect of anions on both phenomena—effect of inorganic additives on solutions of nonionic surfactants. 8 *Tenside. Surfact. Det.* **34** 304–14
[35] Rosseinsky D R and Mortimer R J 2001 Electrochromic systems and the prospects for devices *Adv. Mater.* **13** 783–6
[36] Levy D 1997 Photochromic sol–gel materials *Chem. Mater.* **9** 2666–70
[37] Palgrave R G and Parkin I P 2004 Aerosol assisted chemical vapour deposition of photochromic tungsten oxide and doped tungsten oxide thin films *J. Mater. Chem.* **14** 2864–7